21cm-LAE cross-correlationによる宇宙再電離期の観測可能性の調査

久保田賢志(熊本大学)

<u>共同研究者</u>

吉浦伸太郎(熊本大学)

高橋慶太郎(熊本大学)

長谷川賢二(名古屋大学)

大内正己(東京大学・宇宙線研)

Ongoing 21cm observation

MWA(Australia) LOFAR(Netherland) PAPER(South Africa)

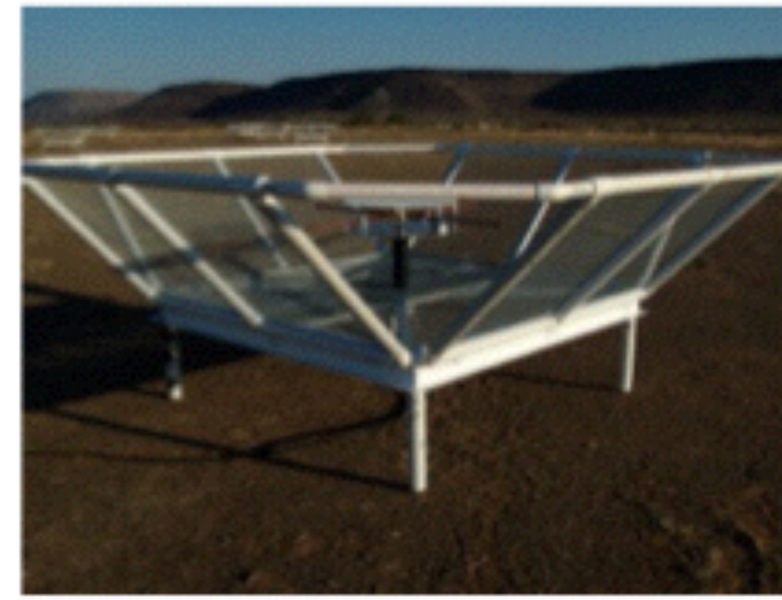

	MWA	LOFAR	PAPER
frequency	80-300MHz	30-80MHz 120-240MHz	100-200MHz
frequency resolution	~40kHz	~0.8kHz	~97.6kHz
angular resolution	~2arcmin	~2arcmin	~0.3deg
field of view(FoV)	~20×20deg^2	~3×3deg^2	~1×1deg^2

Future 21cm observation

SKA1-Low(Australia)

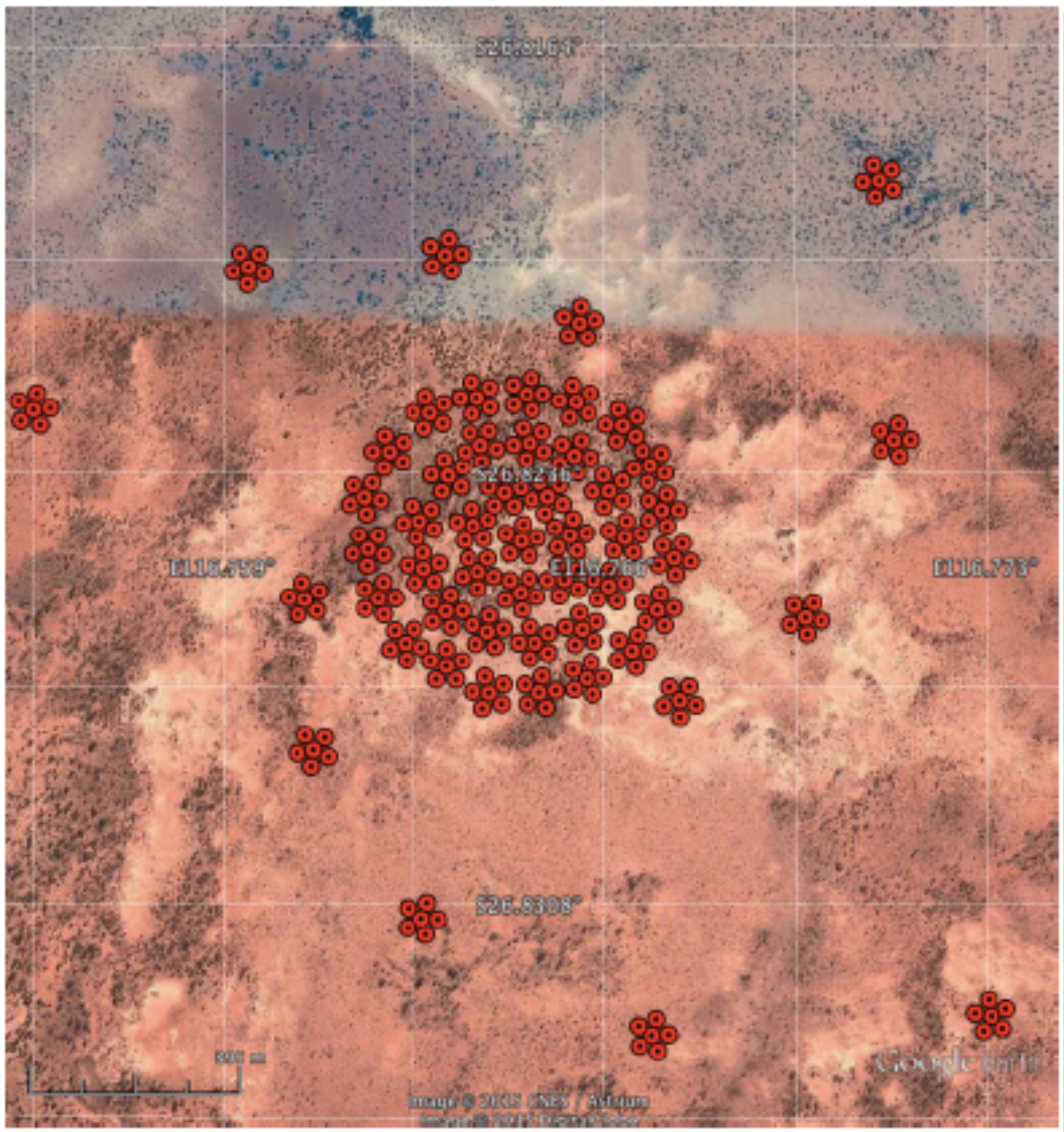

frequency	50-350MHz
frequency resolution	~1kHz
angular resolution	~1arcmin
field of view	>4×4deg^2
maximum base line length	~700m

Problem of 21cm-line observation

Jelic 2008

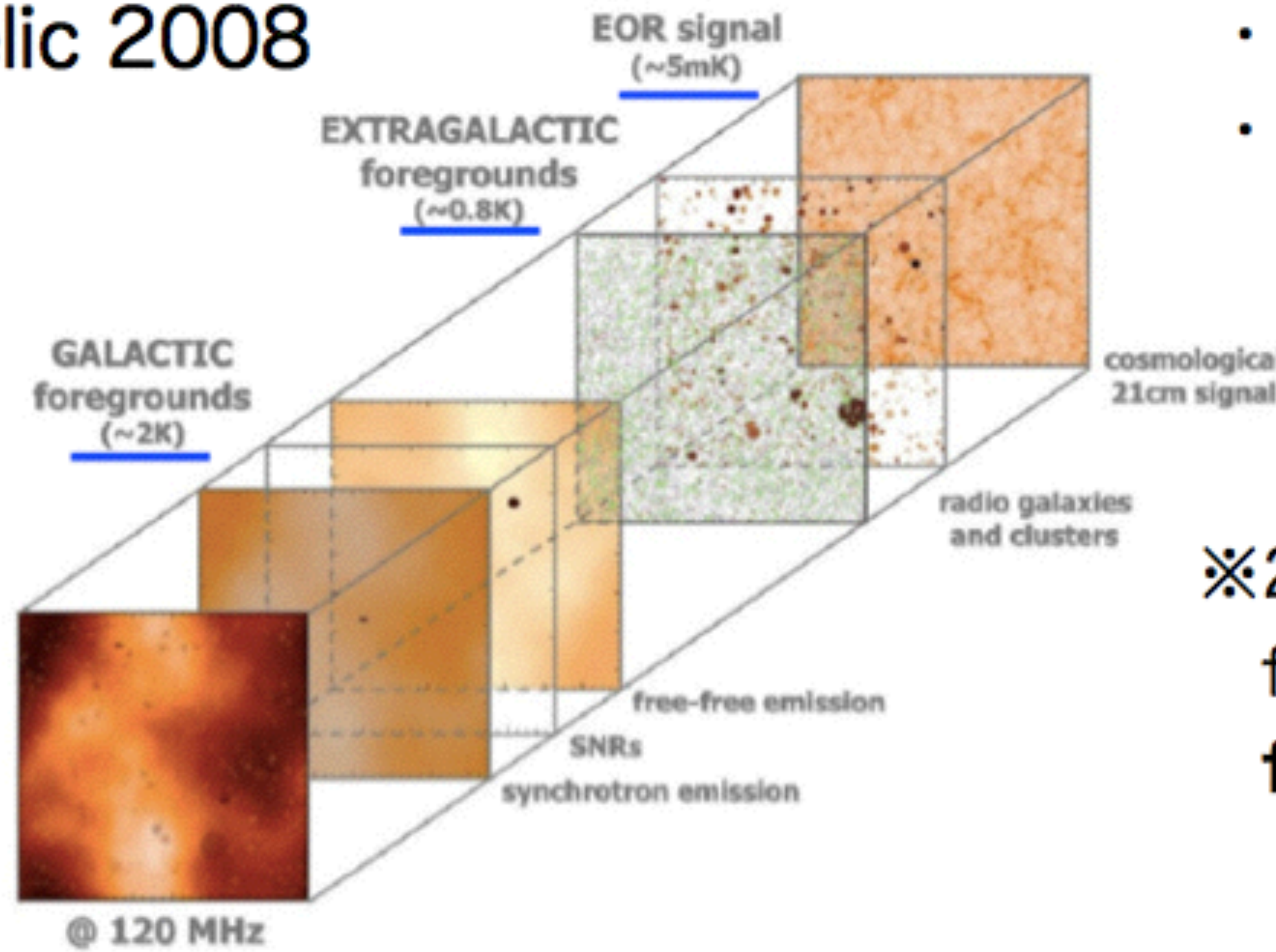

Foreground

- galactic synchrotron
- extragalactic radio

etc…

※21cm signal : ~mK
foreground : ~K
foreground >> 21cm

The detection of 21cm signal is very challenging!

→We focused on the correlation with 21cm and galaxy.

Image of the cross-correlation

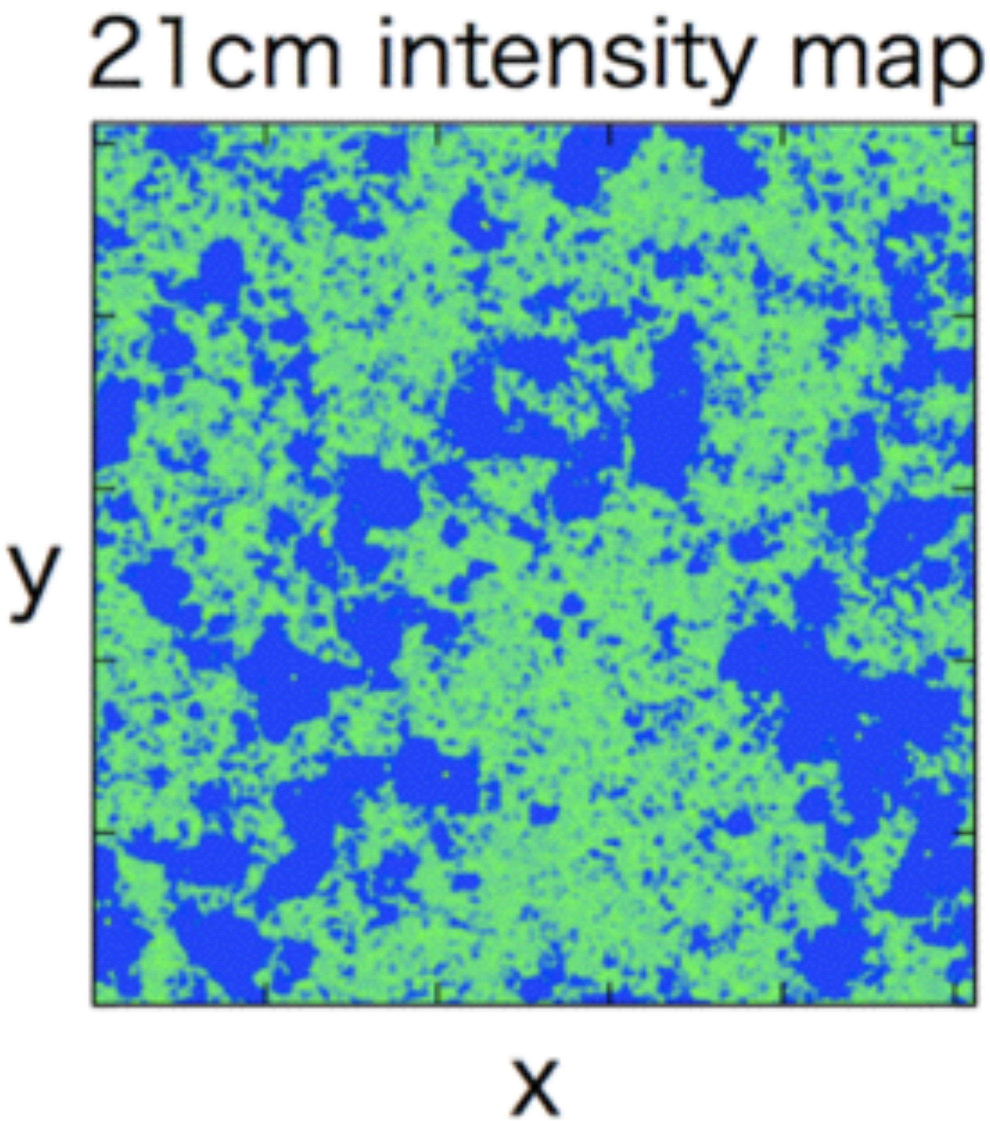

$\times$

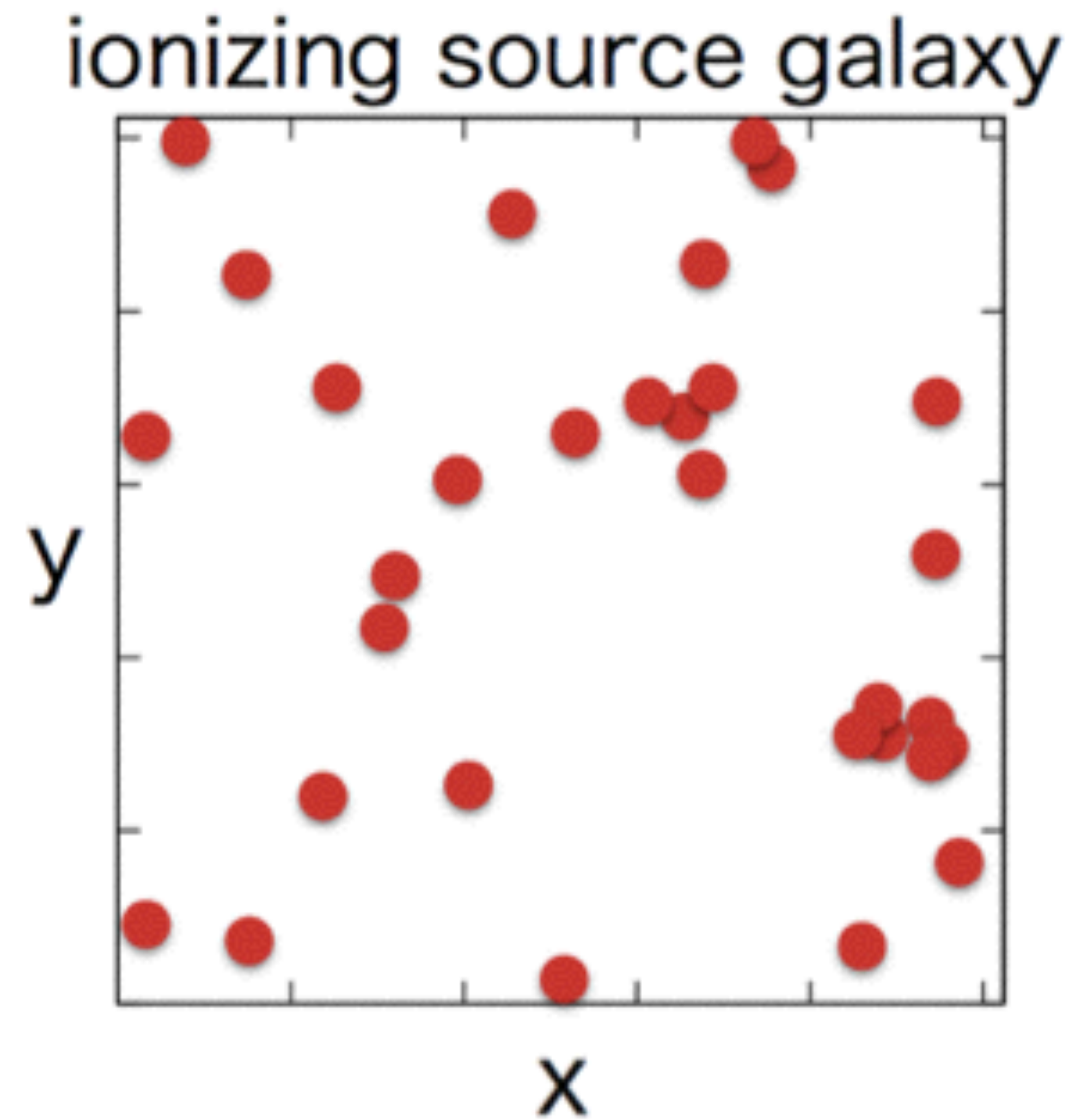

Galaxies reside in ionized regions.

No galaxy regions are neutral.

$\Longrightarrow$ anti-correlation

21cm-galaxy cross-correlation

$$\left\langle \hat{\delta}_{21}(\mathbf{k}_1)\hat{\delta}_{\rm gal}(\mathbf{k}_2)\right\rangle \equiv (2\pi)^3\delta_D(\mathbf{k}_1+\mathbf{k}_2)\underbrace{P_{21,\rm gal}(\mathbf{k}_1)}_{\text{cross-power spectrum}},$$

We perform both 21cm observation and galaxy survey.

21cm observation $\cdots$ $\delta_{21} = \delta_{21\rm sig} + \delta_{21\rm noise} + \delta_{21\rm FG}$

galaxy survey $\cdots$ $\delta_{\rm gal} = \delta_{\rm gal\ sig} + \delta_{\rm gal\ noise}$

$$\langle\delta_{21}\delta_{\rm gal}\rangle = \langle\delta_{21\rm sig}\delta_{\rm gal\ sig}\rangle + \cdots + \underbrace{\langle\delta_{21\rm FG}\delta_{\rm gal\ sig}\rangle}_{\sim 0} + \underbrace{\langle\delta_{21\rm FG}\delta_{\rm gal\ noise}\rangle}_{\sim 0}$$

21cm signal is correlated with galaxy distribution.
FG in 21cm is non-correlated with galaxy survey.

→ We expect the detection of 21cm signal.

Lyman-α emitter(LAE)

- high-z galaxy bright in Lymanα-line
- one of the ionizing sources
- narrow band survey by HSC @z=6.6, 7.3
- Ultra Deep, Deep field → 2D cross-correlation

  $\Delta z \sim 0.1$
- +PFS → 3D cross-correlation

  $\Delta z \sim 0.0007$

◎Check qualitative feature of cross-spectrum under our realistic IGM simulation

→ Hasegawa et al. 2016(1603.01961)

◎Detectability of 2D and 3D cross-spectrum

⇒ ・Comparison ultra deep with deep field

・necessity of PFS

LAE modeling

Table 1: **Summary of HSC-Wide, Deep and Ultradeep layers**

Layer	Area [deg^2]	# of HSC fields	Filters & Depth	Comoving volume [h^{-3}Gpc^3]	Key Science
Wide	1400	916	*grizy* ($r \simeq 26$)	$\sim 4.4\,(z < 2)$	WL cosmology, $z \sim 1$ gals, clusters
Deep	27	15	*grizy*+3NBs ($r \simeq 27$)	$\sim 0.5\,(1 < z < 5)$	$z \lesssim 2$ gals, reionization, WL calib.
Ultradeep	3.5	2	*grizy*+3NBs ($r \simeq 28$)	$\sim 0.07\,(2 < z < 7)$	$z \gtrsim 2$ gals, reionization, SNeIa

Table 6: LAE and LAB Samples

narrow-band	NB387	NB816^a	NB921^a	NB101^a
redshift	2.18 ± 0.02	5.71 ± 0.05	6.57 ± 0.05	7.30 ± 0.04
$N^b_{\rm UD}$	–	3.9k (60)	1.7k (30)	39 (0)
$N^b_{\rm D}$	9.0k (730)	14k (360)	5.5k (100)	–
$V^c_{\rm UD}$	–	1.2	1.2	0.79
$V^c_{\rm D}$	6.0	9.6	9.8	–
$L({\rm Ly}\alpha)^d_{\rm UD}$	–	1.5	2.5	6.8
$L({\rm Ly}\alpha)^d_{\rm D}$	2.7	2.9	4.1	–
science^e	LA	LA, CR	LA, CR	LA, CR

Notes – $^{a)}$ We will use these narrow-band data down to the 4σ limits, following the convention in the literature. $^{b)}$Expected number of LAEs, with numbers of LABs in parentheses, in each redshift slice. $^{c)}$The comoving volume of each redshift slice in units of $10^6(h^{-1}{\rm Mpc})^3$. $^{d)}$Limiting Lyα luminosity in units of 10^{42} erg s^{-1}. $^{e)}$Key science cases. LA: evolution of LAEs and LABs (Section 5.2), CR: cosmic reionization (Section 5.4).

21cm-LAE cross-power spectrum

$$\left\langle \hat{\delta}_{21}(\mathbf{k}_1)\hat{\delta}_{\rm gal}(\mathbf{k}_2) \right\rangle \equiv (2\pi)^3 \delta_D(\mathbf{k}_1 + \mathbf{k}_2) P_{21,\rm gal}(\mathbf{k}_1),$$

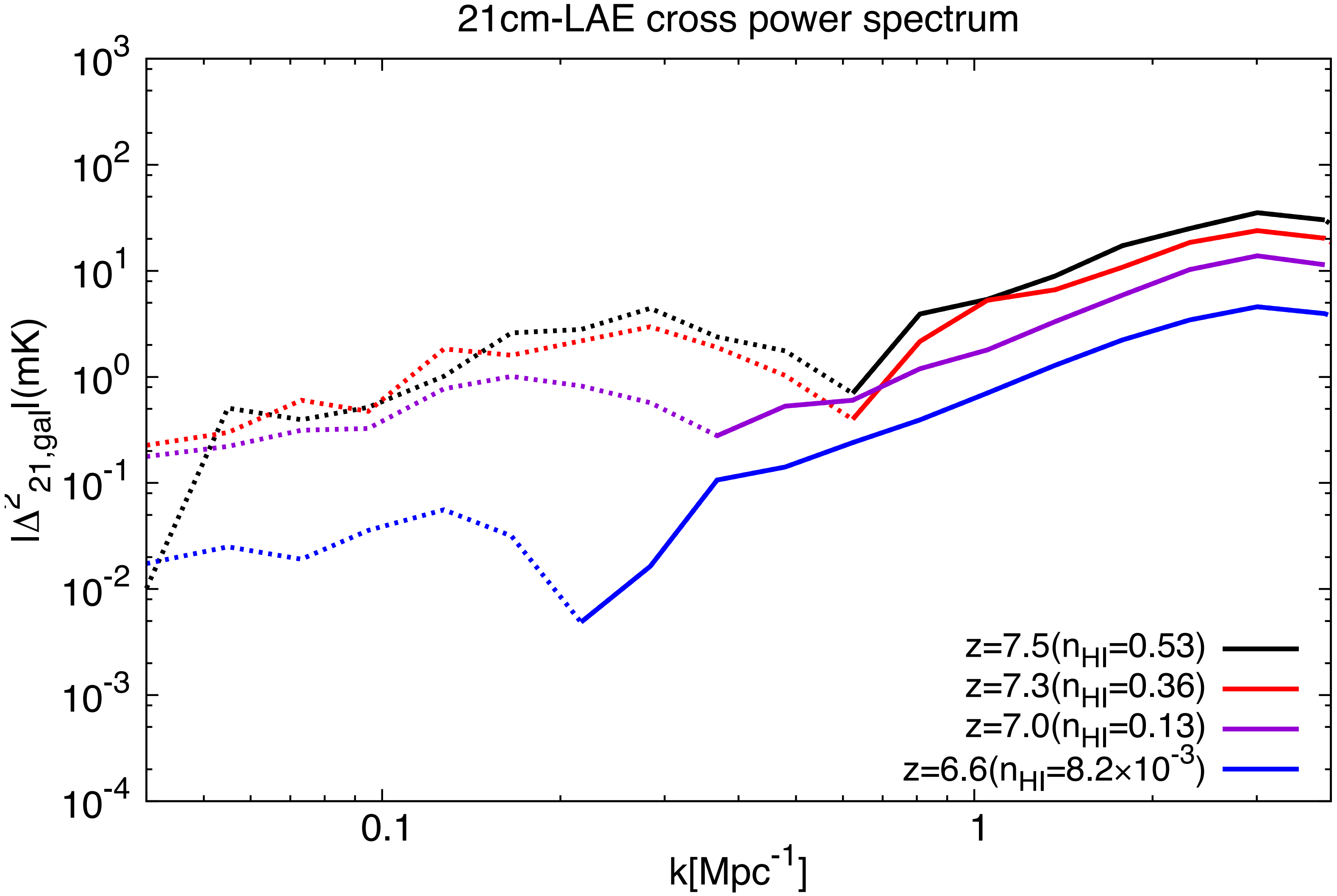

- negative on large scale
- sign changes in a scale

Turnover scale depends on redshift.

Turnover scale corresponds to size of ionized bubble.

We could confirm the basic feature in previous study under our realistic simulations.

Detectability

Furlanetto & Lidz(2007)

※ $k_{\parallel} = \mu k$

$$\sigma_A^2(k,\mu) = \mathrm{var}\left[P_{21,\mathrm{gal}}(k,\mu)\right]$$
$$= \frac{1}{2}\left[\underbrace{P_{21,\mathrm{gal}}^2(k,\mu)}_{\text{sample variance}} + \sigma_B(k,\mu)\sigma_C(k,\mu)\right],$$

$$\sigma_B^2(k,\mu) = \mathrm{var}\left[P_{21}(k,\mu)\right]$$
$$= \left[\underbrace{P_{21}(k,\mu)}_{\text{sample variance}} + \underbrace{\frac{T_{\mathrm{sys}}^2}{T_0^2}\frac{1}{Bt_{\mathrm{int}}}\frac{D^2\Delta D}{n(k_\perp)}\left(\frac{\lambda^2}{A_e}\right)^2}_{\text{thermal noise}}\right]^2,$$

$$\sigma_C^2(k,\mu) = \mathrm{var}\left[P_{\mathrm{gal}}(k,\mu)\right]$$
$$= \left[\underbrace{P_{\mathrm{gal}}(k,\mu)}_{\text{sample variance}} + \underbrace{n_{\mathrm{gal}}^{-1}e^{k_{\parallel}^2\sigma_\chi^2}}_{\text{shot noise, redshift error}}\right]^2.$$

$$\frac{1}{\sigma_A^2(k)} = \sum_{\mu}\frac{\epsilon k^3 V_{\mathrm{survey}}}{4\pi^2}\frac{\Delta\mu}{\sigma_A^2(k,\mu)}.$$: variance on cross-spectrum

MWA-ultra deep

MWA : 1000h, 256tiles
ultra deep : 3.5deg^2, σ_z=0.1(=Δz)
ultra deep+PFS : 3.5deg^2, σ_z=0.0007

z=6.6(f_HI=8.2×10^-3)

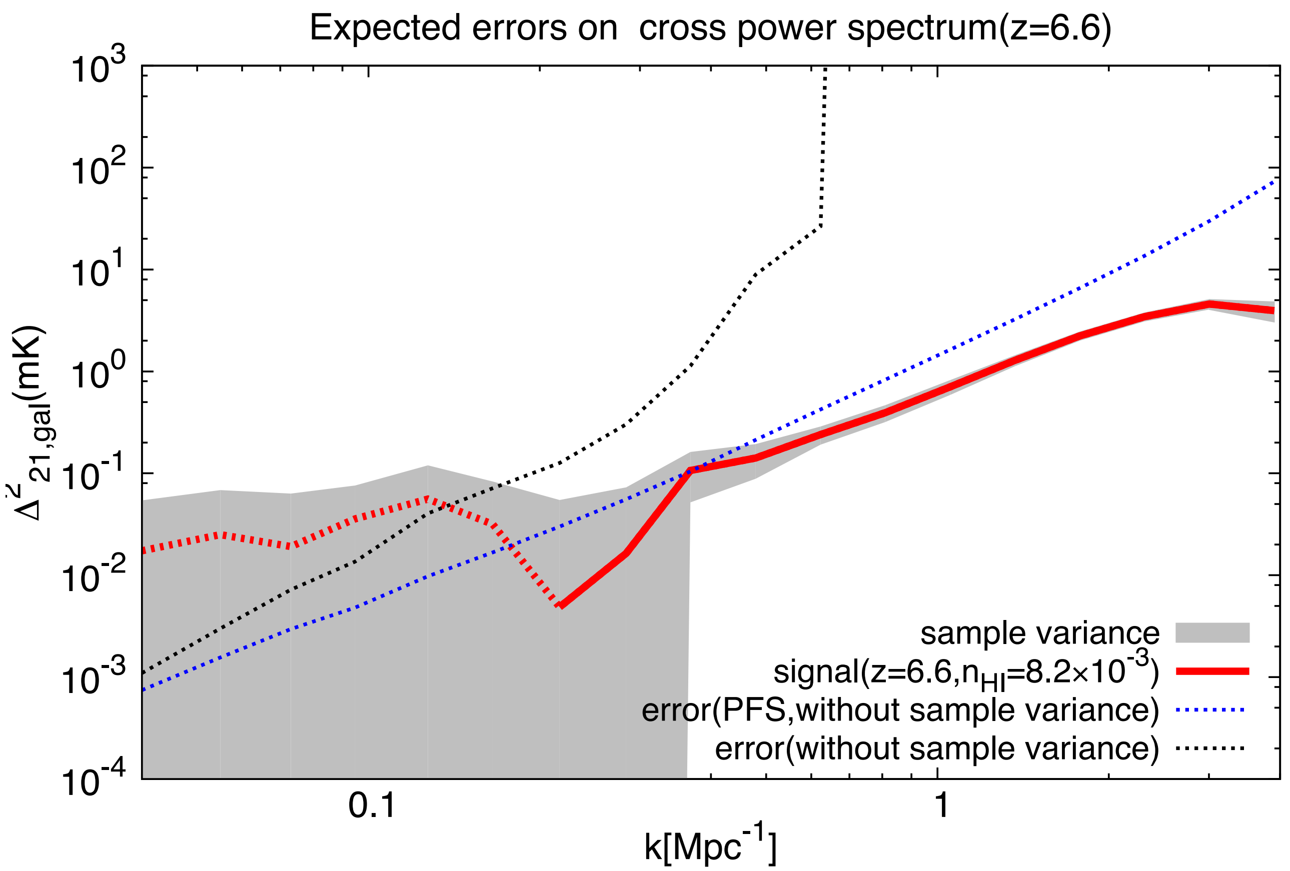

z=7.3(f_HI=0.36)

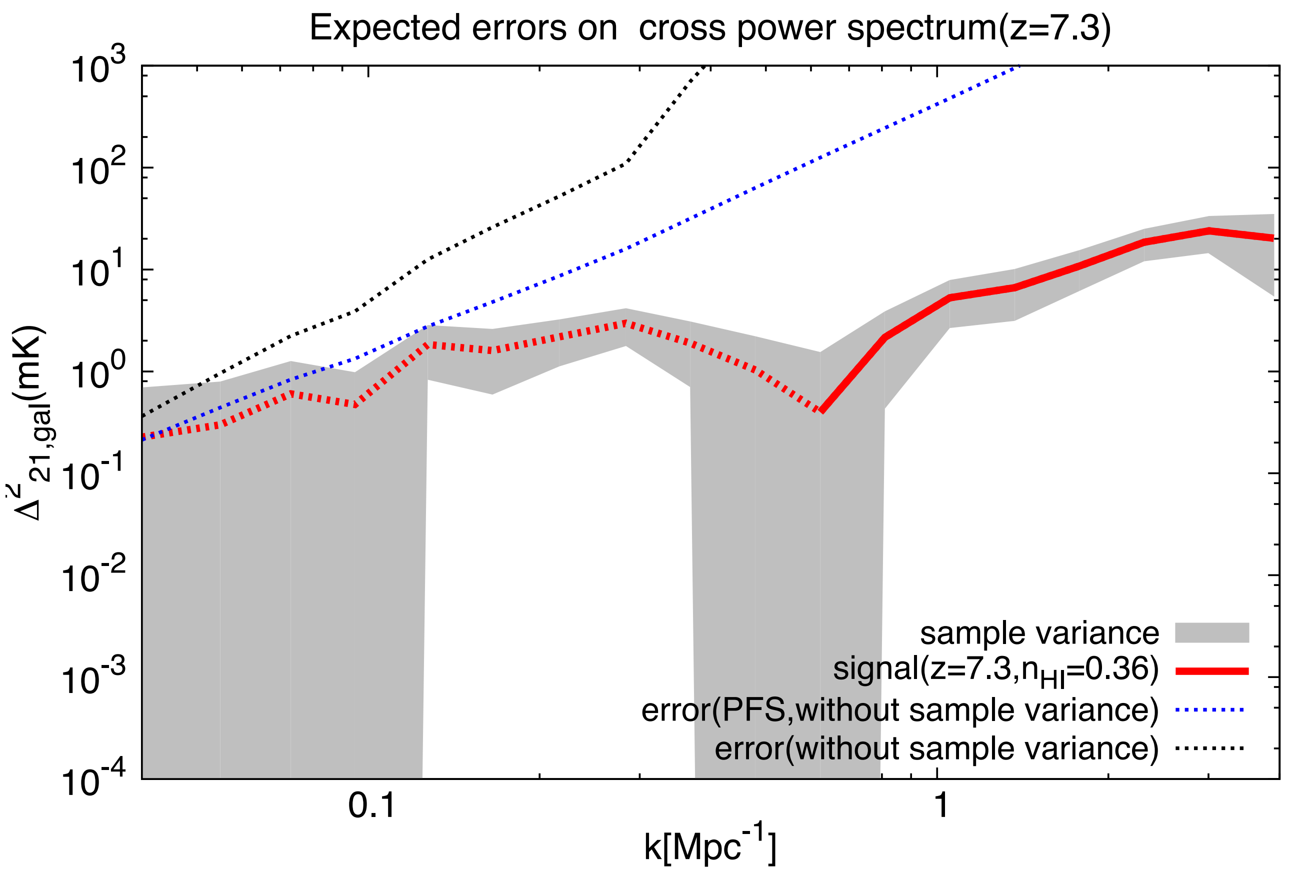

Depending on sample variance,
detectable at large scale@z6.6

red : signal
blue : error(ultra deep+PFS)
black : error(ultra deep)

SKA1-ultra deep

SKA1 : 1000h, 512tiles
ultra deep : 3.5deg^2, σ_z=0.1(=Δz)
ultra deep+PFS : 3.5deg^2, σ_z=0.0007

z=6.6(f_HI=8.2×10^-3)

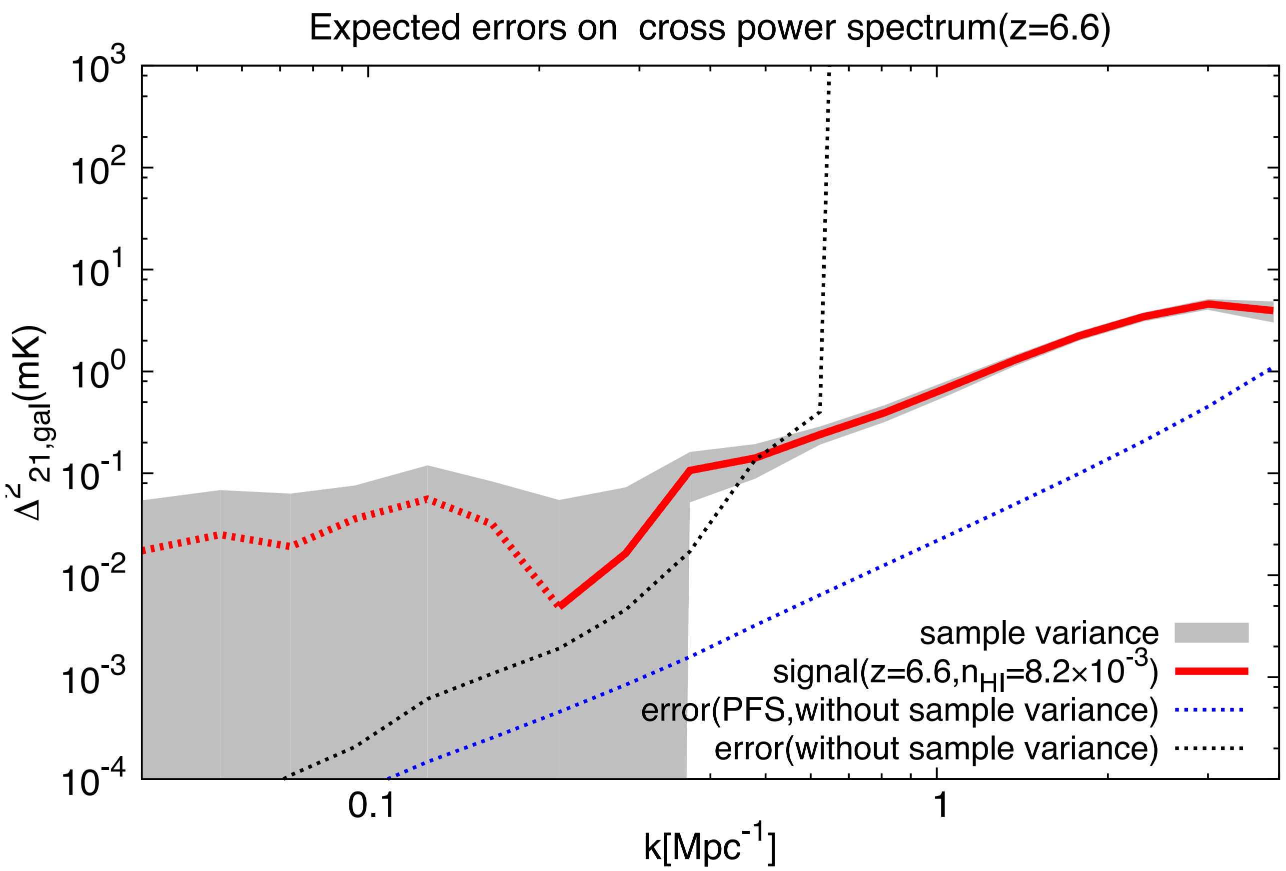

z=7.3(f_HI=0.36)

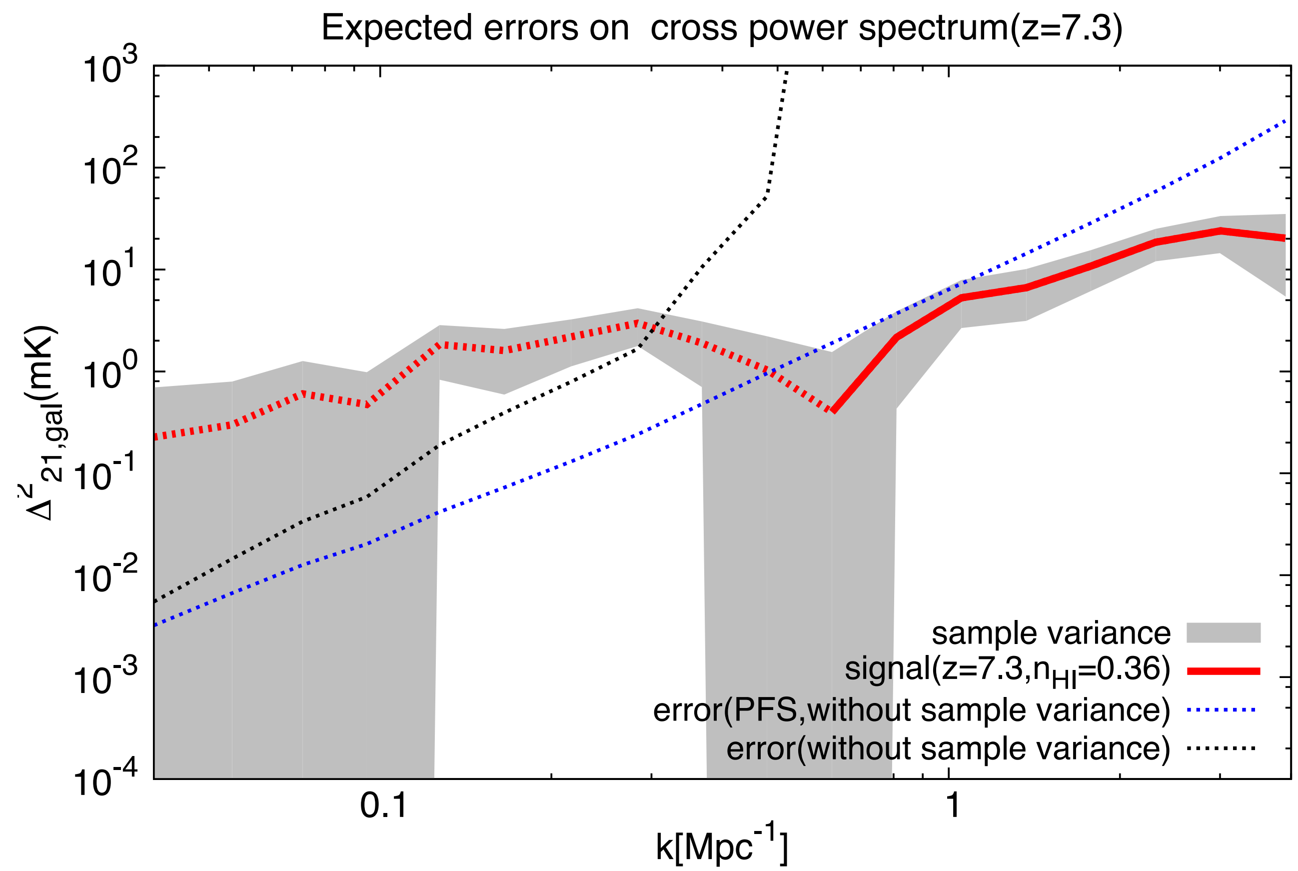

detectable on mid scale@z7.3
PFS is powerful on small scale.

red : signal
blue : error(ultra deep+PFS)
black : error(ultra deep)

※deep : 27deg^2

MWA-deep(z=6.6)

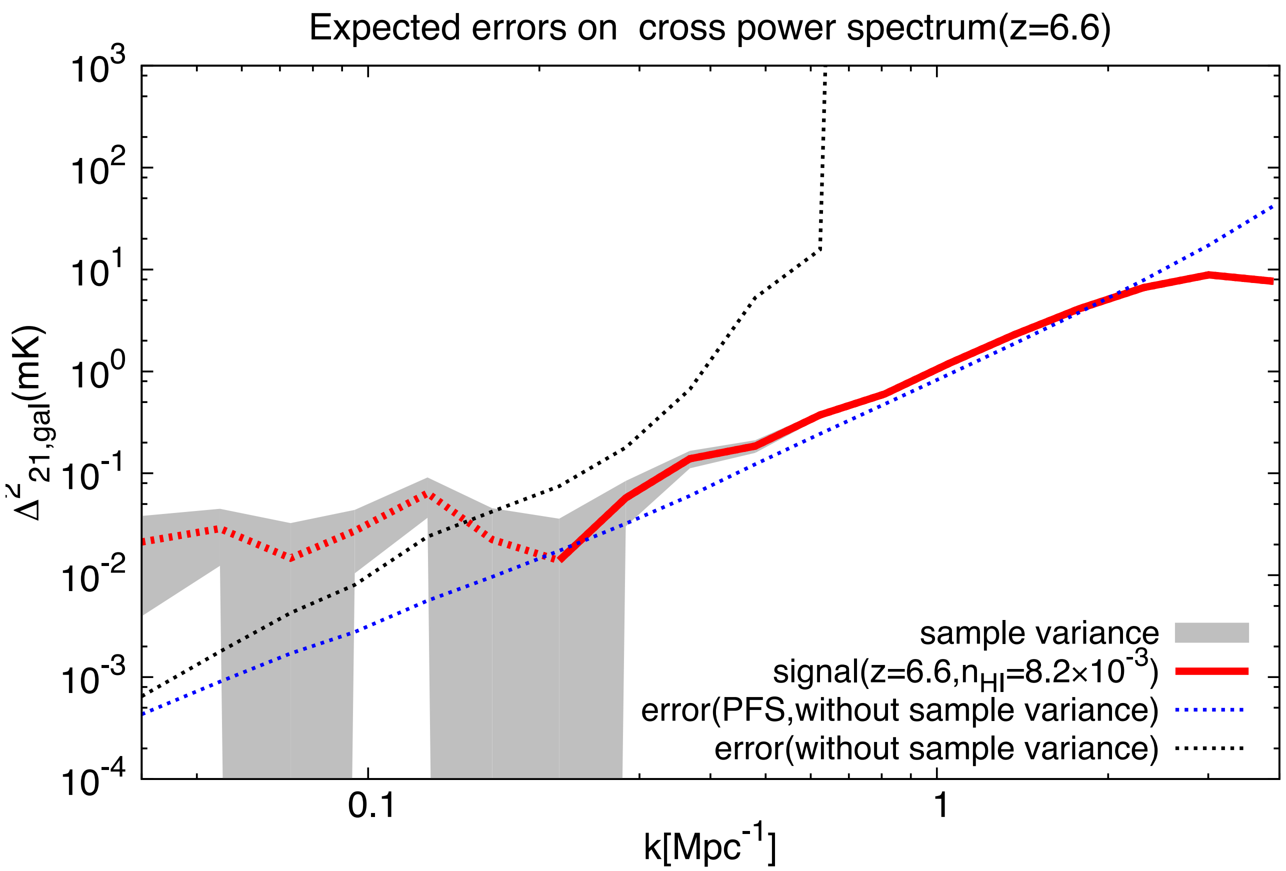

MWA-ultra deep(z=6.6)

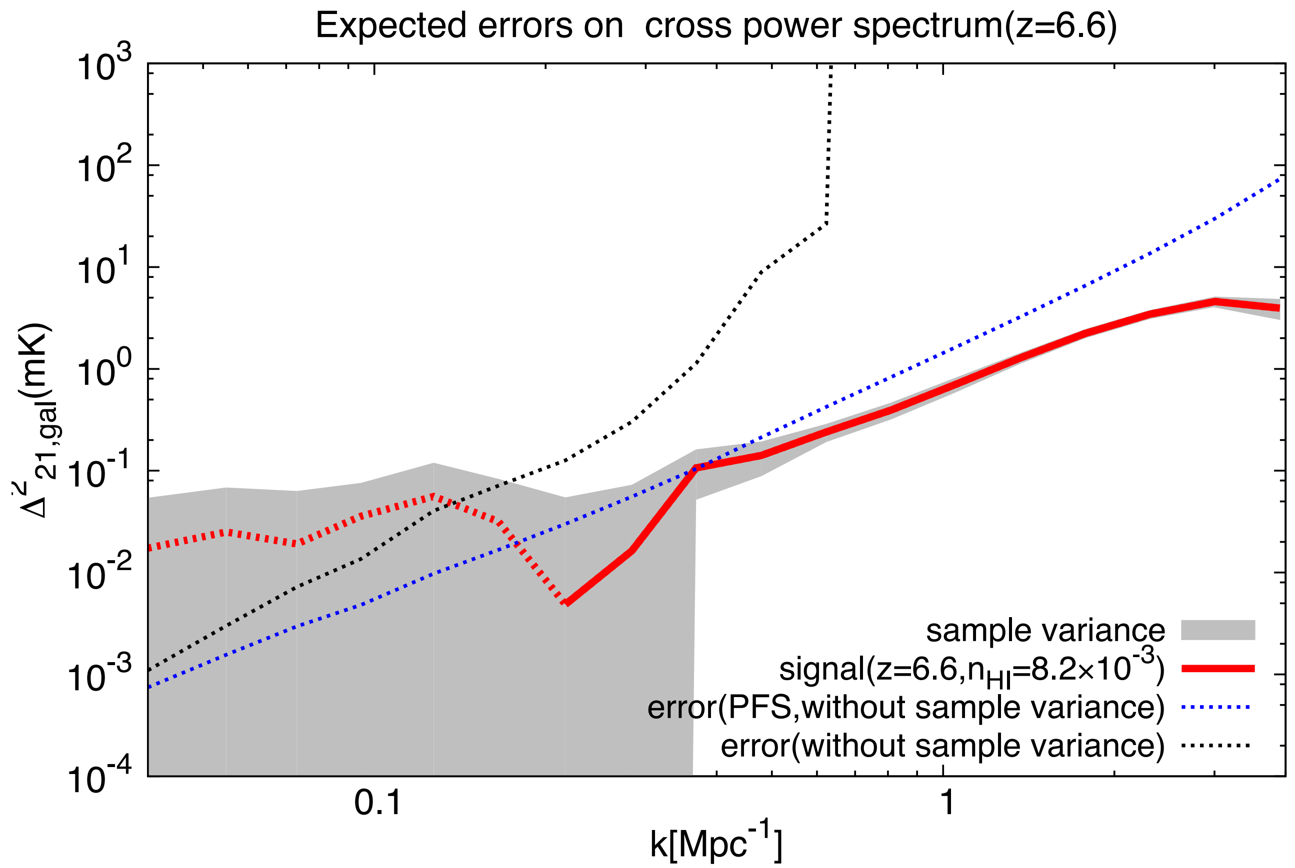

In deep we can detect
the signal on large scale.
→ Deep is advantageous.

red : signal
blue : error(deep+PFS)
black : error(deep)

※deep : 27deg^2

SKA1-deep(z=6.6)

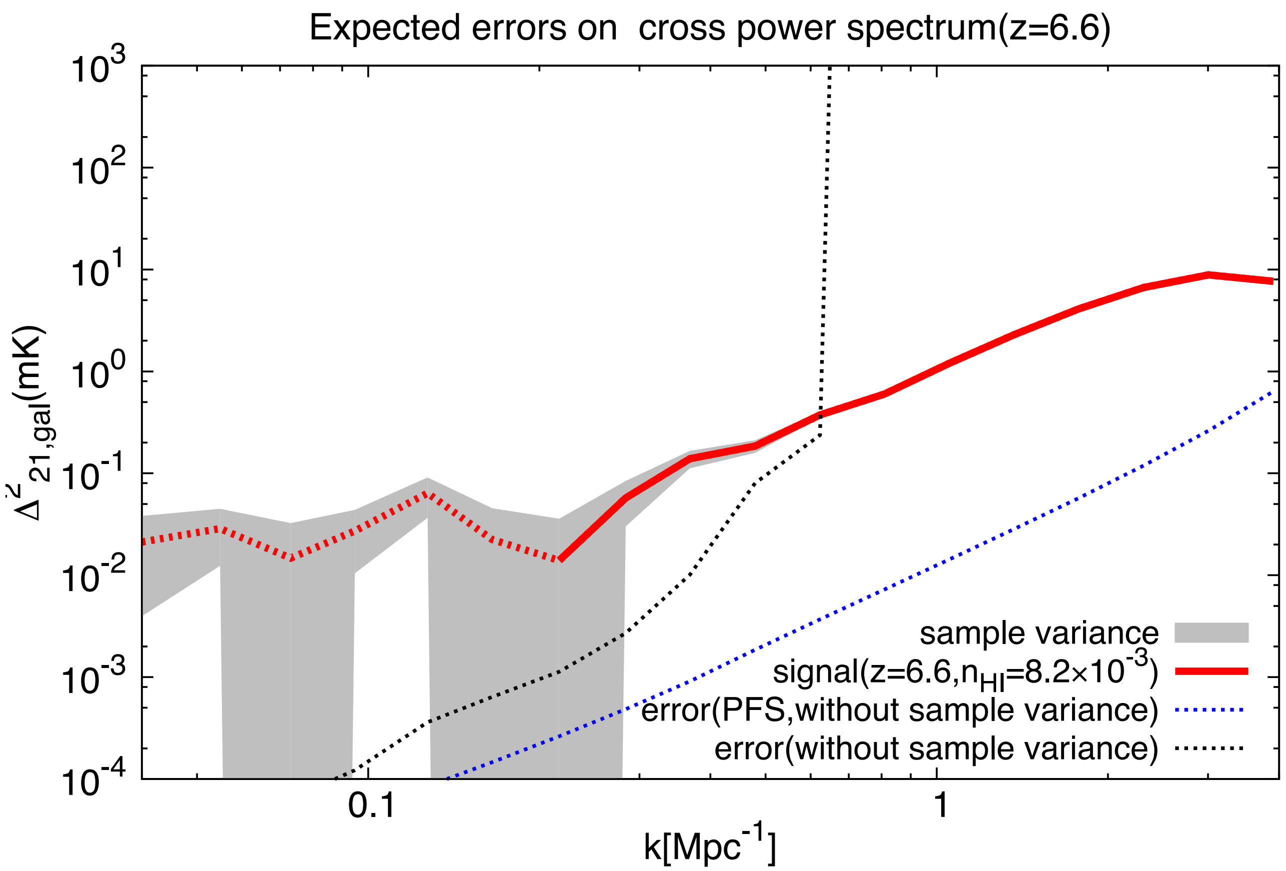

SKA1-ultra deep(z=6.6)

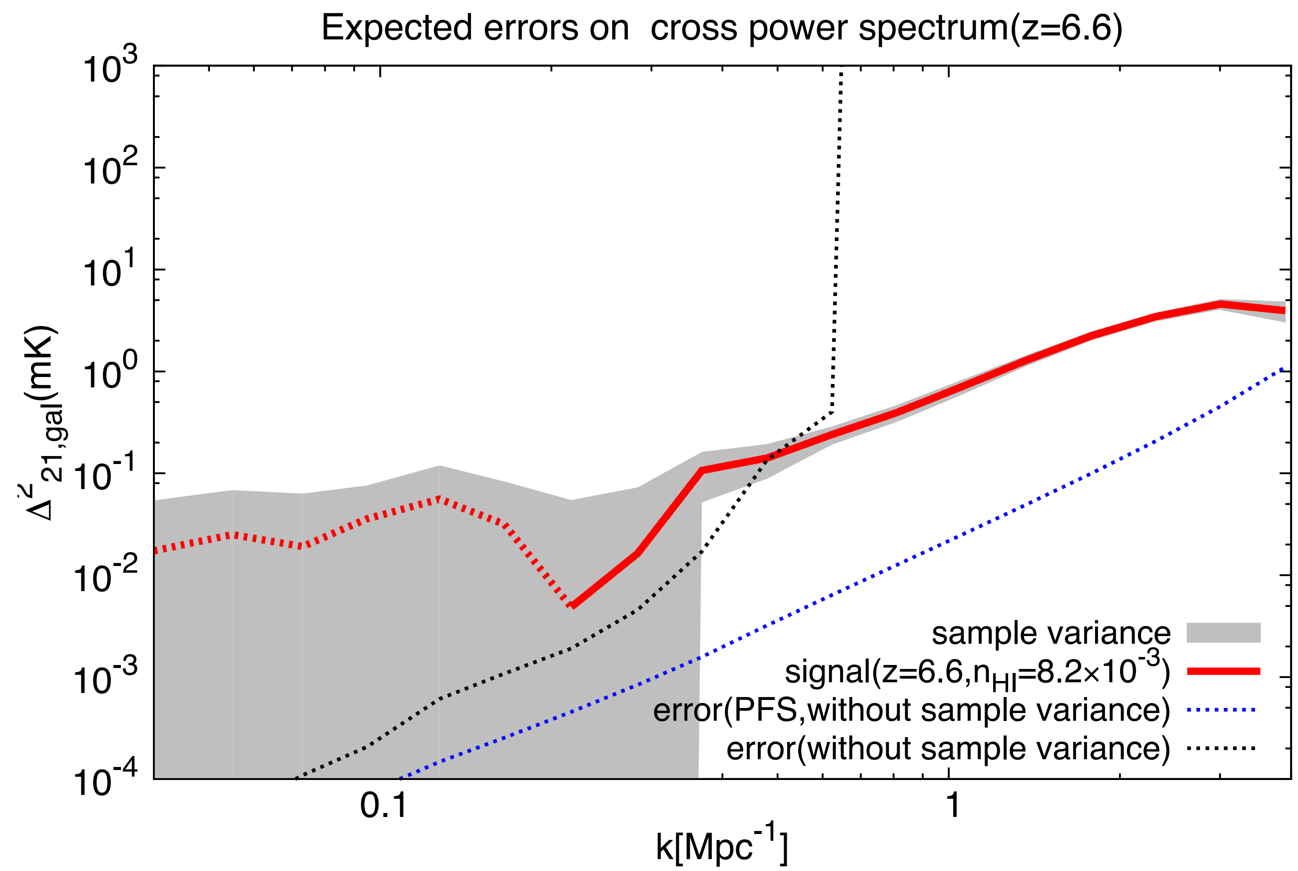

We are likely to see turnover.

red : signal

blue : error(deep+PFS)

black : error(deep)

Comparison of models on MWA-deep(z=6.6)

・mid model(f_HI=8.2×10^-3)

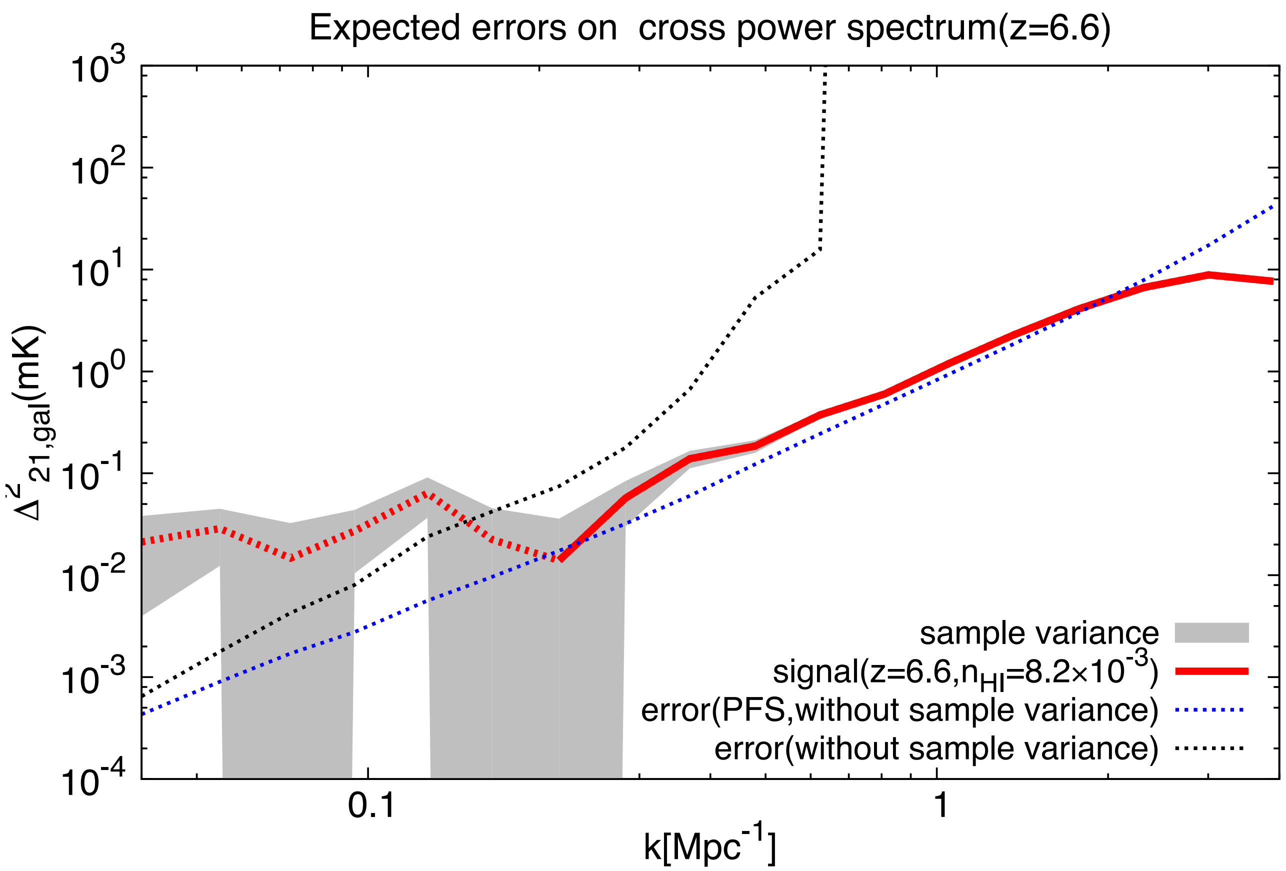

・late model(f_HI=0.11)

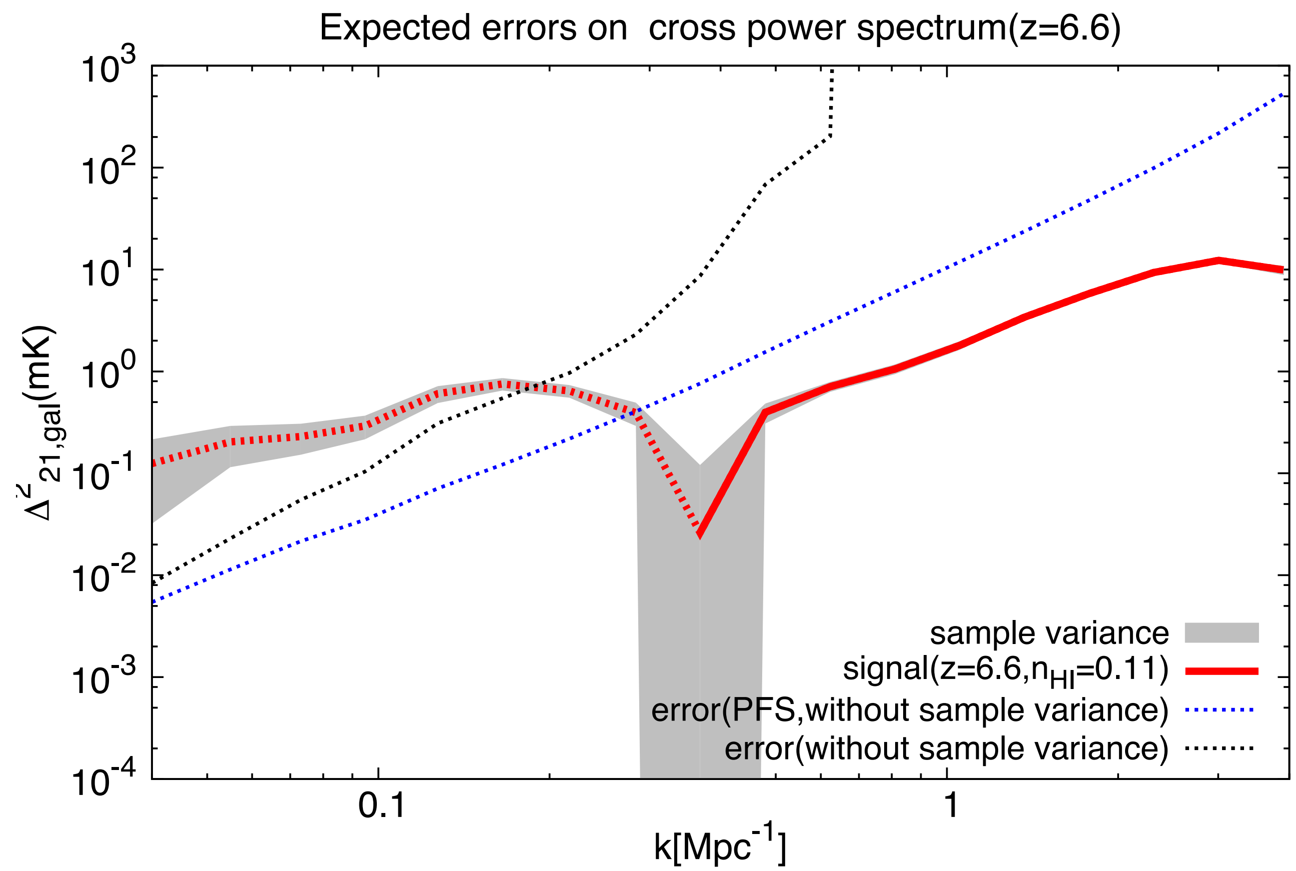

※late model … emissivity/1.5

red : signal

blue : error(deep+PFS)

black : error(deep)

Summary

- Cross-correlation reduces foreground problem.

- We confirm qualitative feature of cross-spectrum
  in our realistic simulation.

- Deep field is advantageous than ultra deep in detection.
  → Survey volume is key to the detection.
  MWA-deep has ability to detect the signal on large scale.

- PFS enhances SKA's ability.
  PFS allows us to detect on small scale.

Back up

・mid model(f_HI=8.2×10^-3)

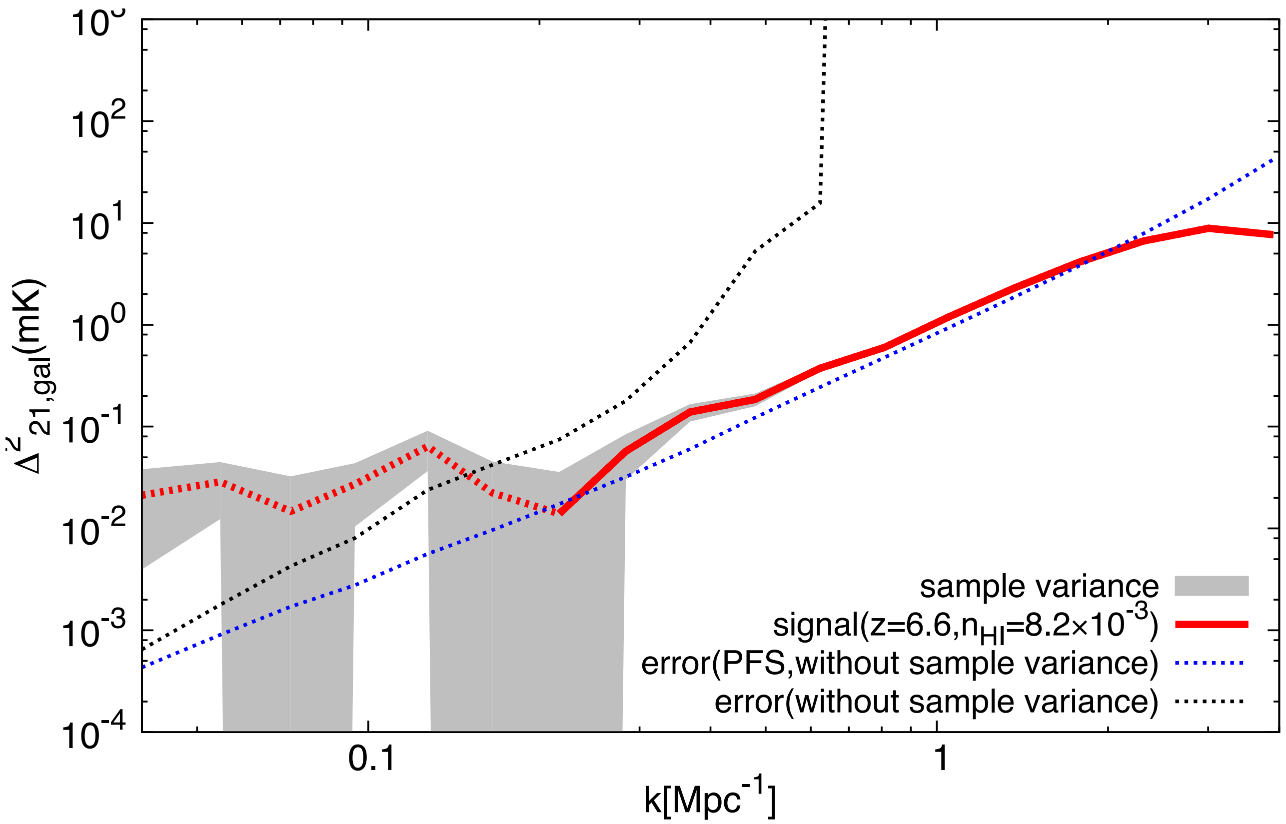

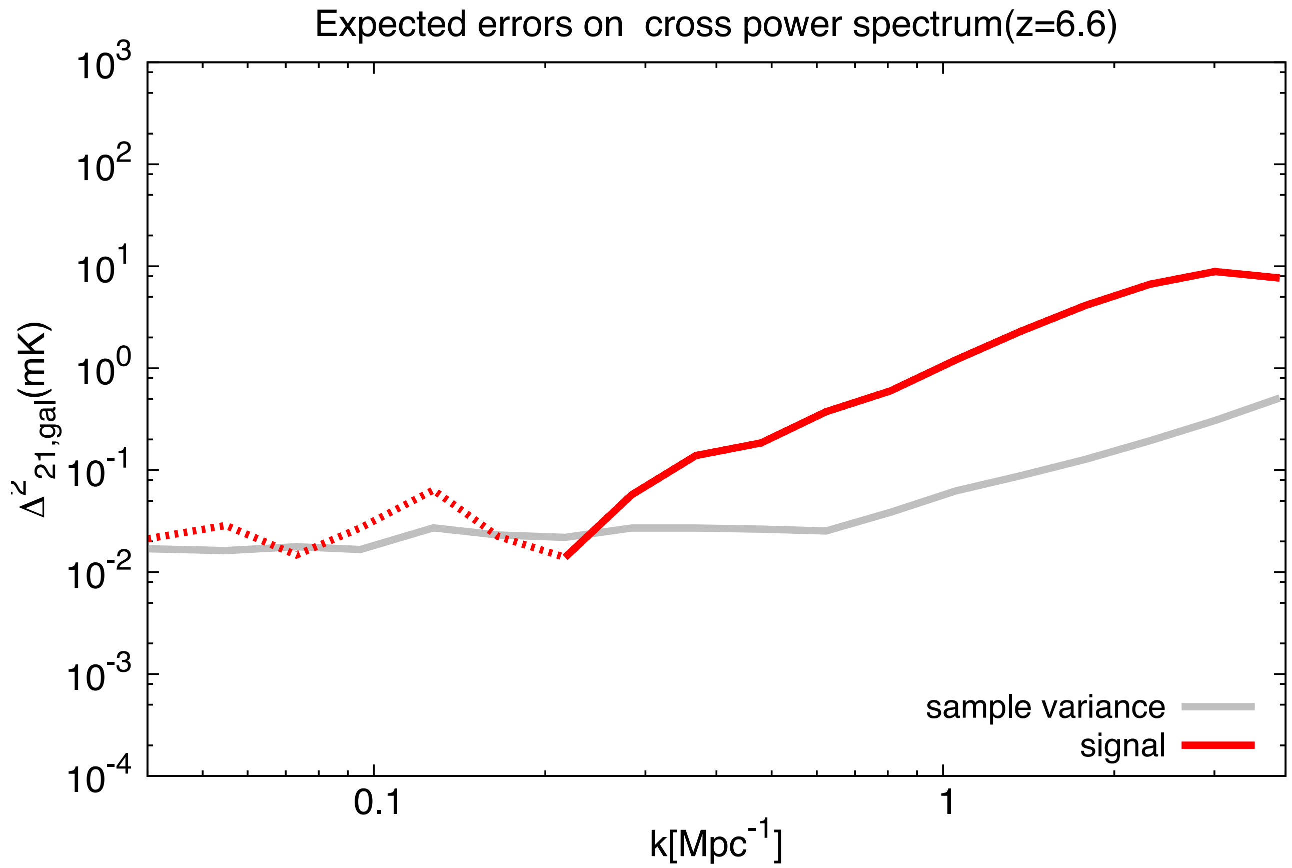

・late model(f_HI=0.11)

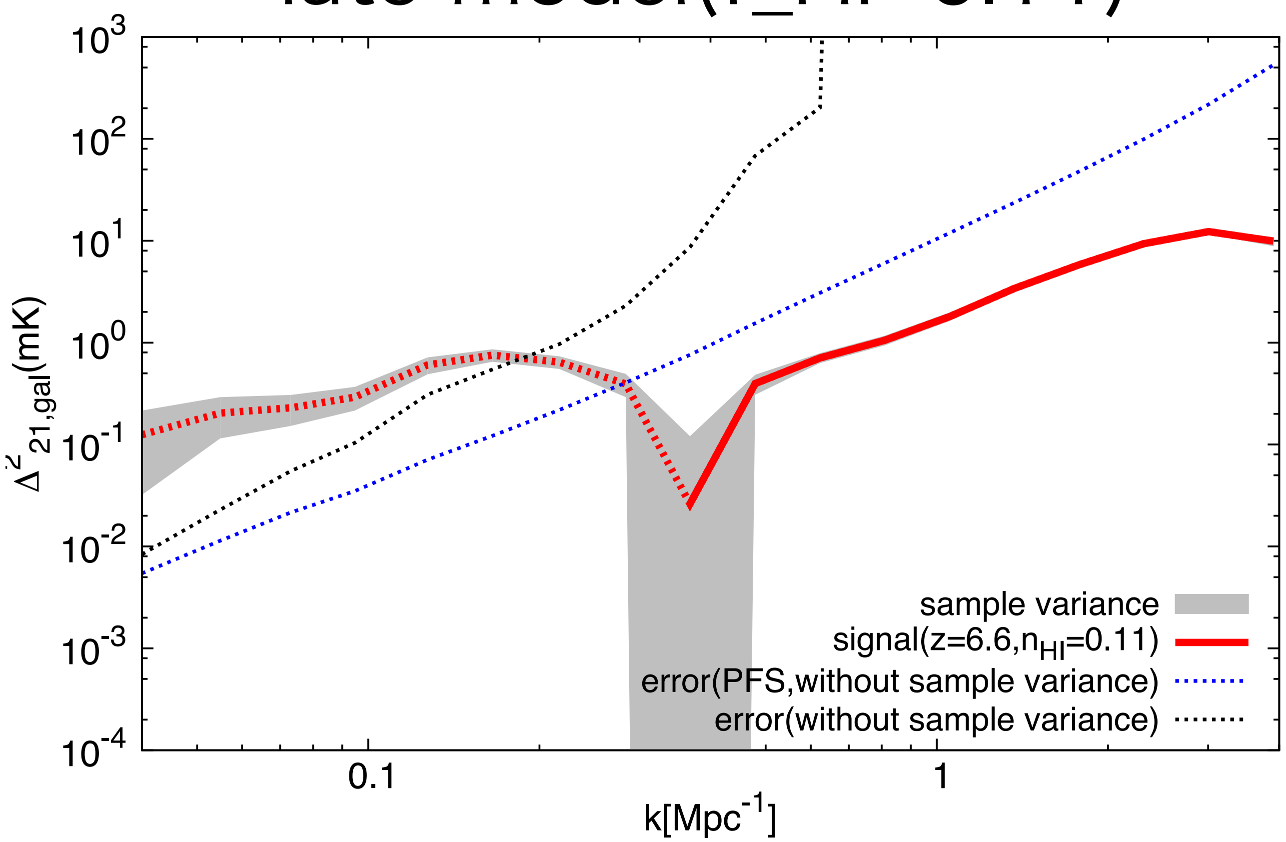

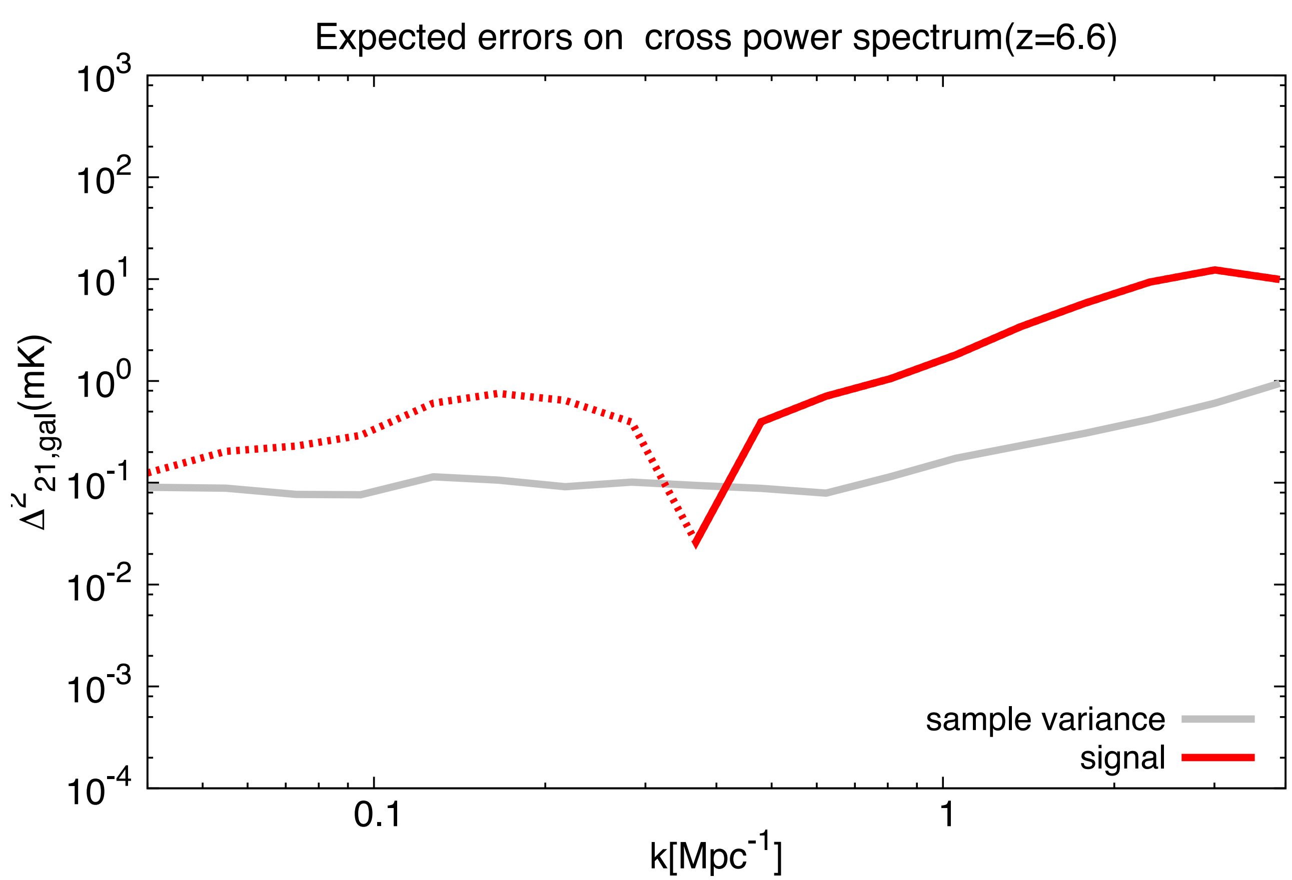

error budget

$$\sigma_A^2 = \frac{1}{2}[P_{21,\mathrm{gal}}^2 + (P_{21} + \sigma_N)(P_{\mathrm{gal}} + \sigma_g)]$$

$$= \frac{1}{2}[\underline{P_{21,\mathrm{gal}}^2} + \underline{P_{21}P_{\mathrm{gal}}} + \underline{P_{21}\sigma_g} + \underline{\sigma_N P_{\mathrm{gal}}} + \underline{\sigma_N\sigma_g}]$$

σ_N : thermal noise

σ_g : shot noise, z error

・mid model(f_HI=8.2×10^-3)

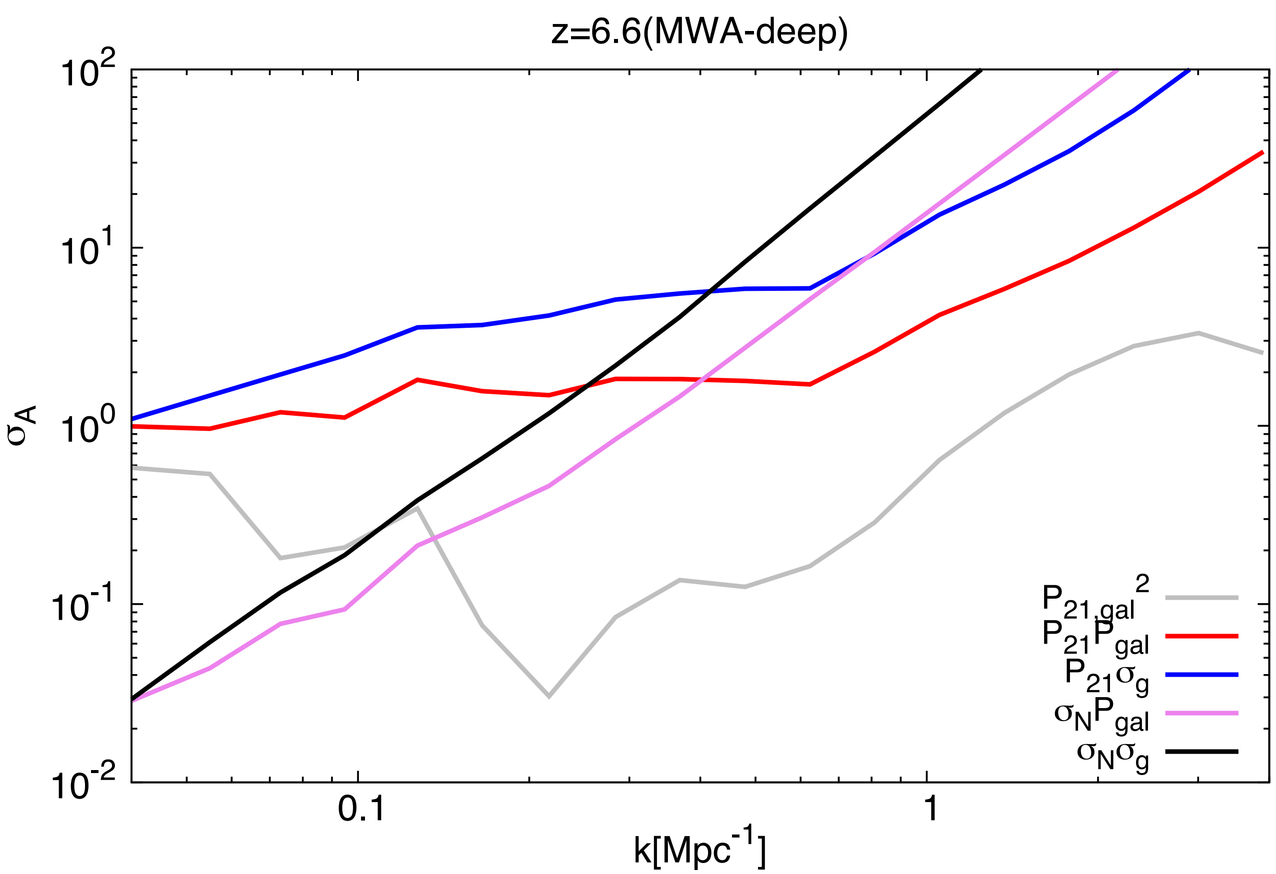

・late model(f_HI=0.11)

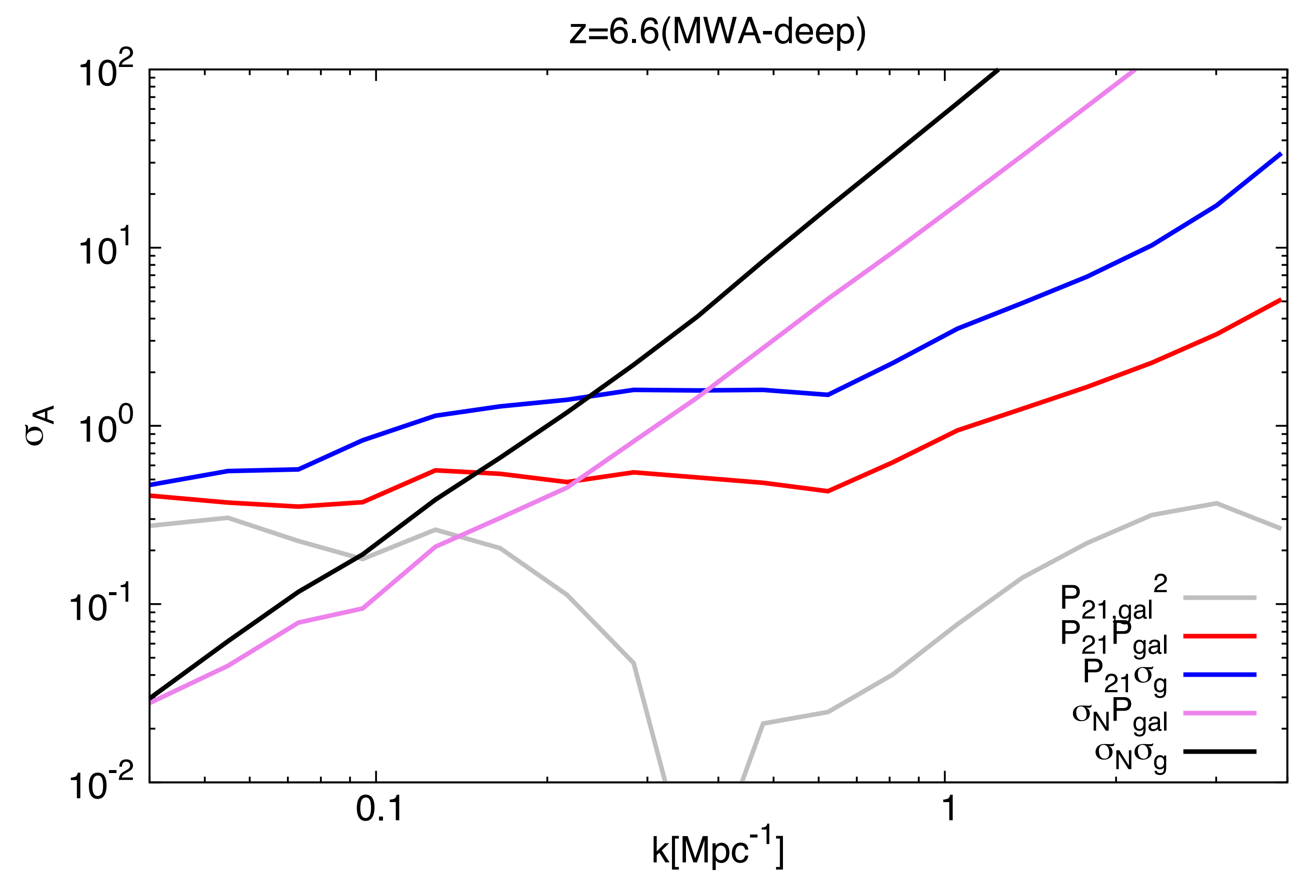

2D cross-power spectrum(z=6.6)   Δz=0.1~40Mpc

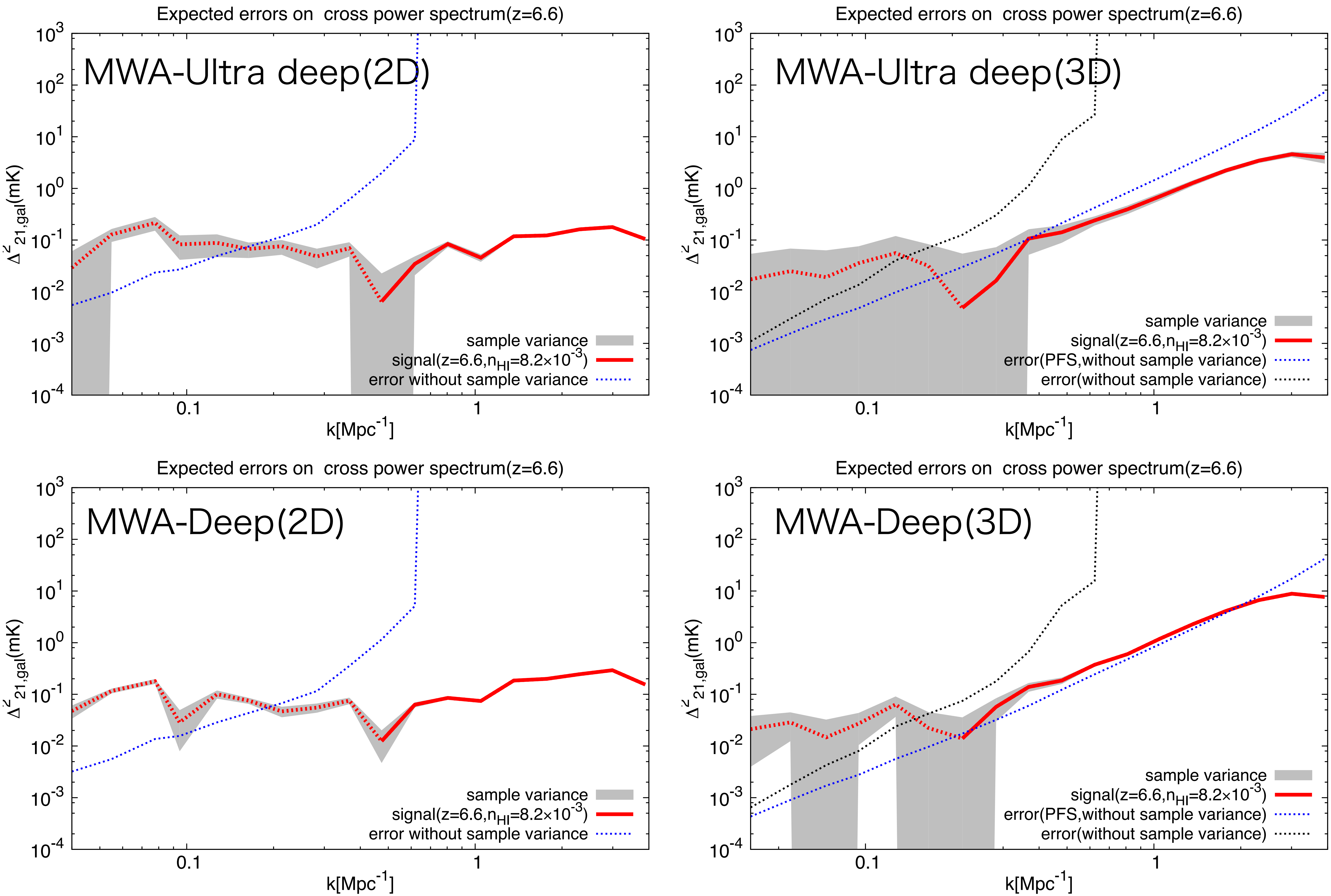

MWA-Deep(2D)

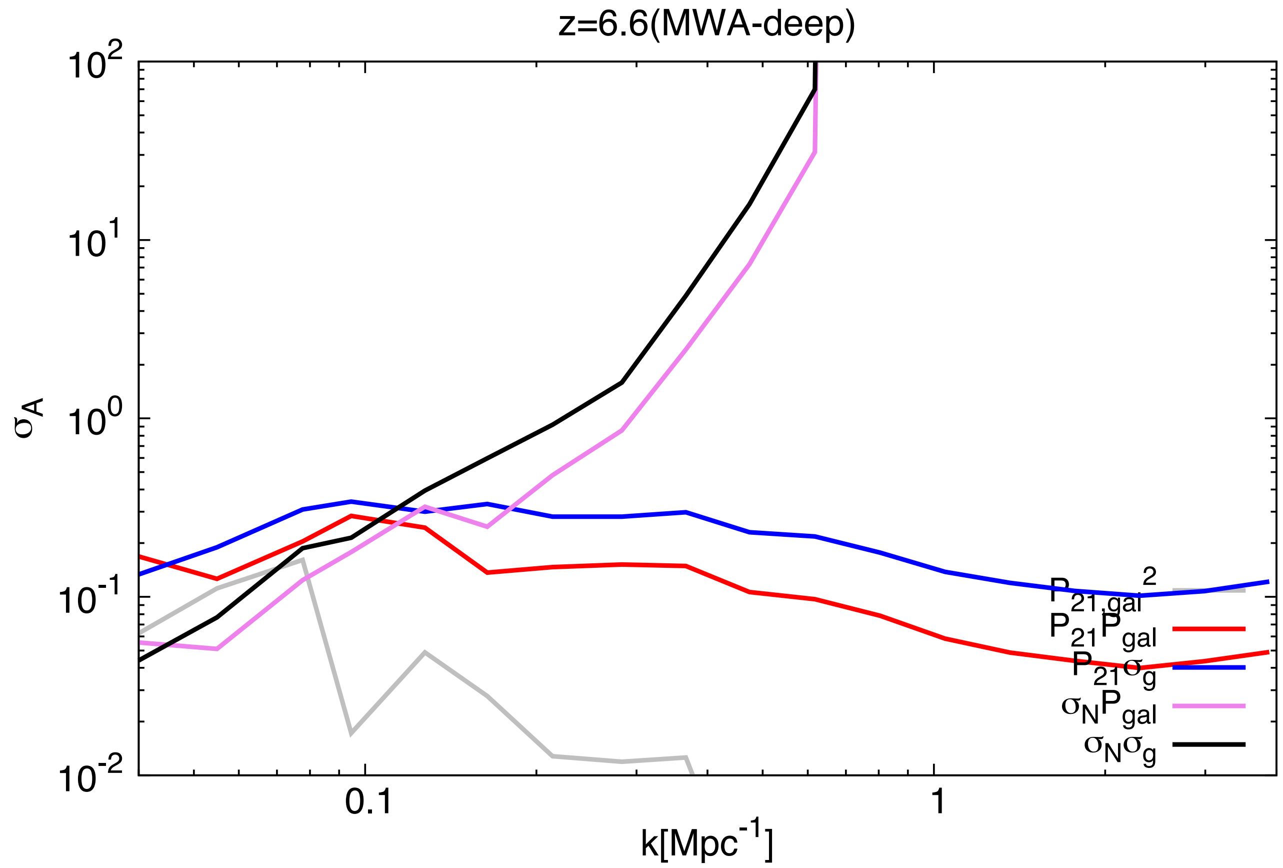

MWA-Deep(3D)